IEEE Access
Multidisciplinary ⋮ Rapid Review ⋮ Open Access Journal

Received September 23, 2020, accepted September 27, 2020, date of publication September 30, 2020,
date of current version October 13, 2020.

Digital Object Identifier 10.1109/ACCESS.2020.3027990

Reduced Modeling of Unbalanced Radial Distribution Grids in Load Area Framework

GIOVANNI MERCURIO CASOLINO, (Member, IEEE), AND ARTURO LOSI
Dipartimento di Ingegneria Elettrica e dell'Informazione "Maurizio Scarano," University of Cassino and Southern Lazio, 03043 Cassino, Italy
Corresponding author: Giovanni Mercurio Casolino (casolino@unicas.it)

This work was supported by the Italian Ministero dell'Istruzione, dell'Università e della Ricerca (MIUR) Program Dipartimenti di Eccellenza 2018–2022.

ABSTRACT A simplified representation of a distribution network offers relevant advantages in limiting the amount of information processed and reducing the computational burden necessary for its treatment, in particular in planning studies, real-time simulations, monitoring and control. The identification of the relevant information for obtaining a correct reduced modeling of a distribution network results from the Load Area (LA) approach. It is based on the concept of groups of nodes/prosumers whose power injection has a similar impact on the operating conditions of distribution grids; the groups are identified through overload and voltage indexes. The paper presents a method for obtaining the reduced equivalent modeling of unbalanced radial grids in the LA framework, once the LAs have been identified. It is based on the backward-forward graph navigation technique for radial grids and a generalization of the modeling of single-phase and two-phase branches. The application and discussion of the method for five different size test cases highlight the computational issues related to the representation and solution of the reduced networks. The results show the feasibility of the proposed method and highlight the computational gains deriving from its adoption.

INDEX TERMS Distribution network reduced modeling, unbalanced systems, backward-forward methods.

NOMENCLATURE

$*$	Reference case/value.
$diag\{x\}$	Diagonal matrix whose elements along the principal diagonal are the components of vector x.
$\dot{\alpha}_{i\_\phi,h}$	1×2 row factor.
$\dot{\alpha}_{i,h}$	3×2 matrix of three factors $\dot{\alpha}_{i\_\phi,h}$.
$\dot{\gamma}_{t,h}$	3×2 matrix for the h-th prosumer's category in the t-th terminal.
$\dot{\theta}_t$	3×3 matrix for the t-th terminal.
$\nu_{h,k}$	Number of phases to which the k–th prosumer of the h–th category is connected.
$\pi_{i\_\phi,h,k}$	Connection to the grid of the k–th prosumer in the h–th category.
$\varphi^*_{h,k}$	Phase angle (assumed constant) of the load current of the k-th prosumer in the h-th category.
$\dot{A}_h$	$n_{LA} \times 2$ matrix whose rows are the factors $\dot{\alpha}_{i\_\phi,h}$.
$\dot{\Theta}_f$	6×6 matrix for the f-th feeder.
$\dot{\Gamma}_{f,h}$	6×2 matrix for the h-th prosumer's category in the f-th feeder.
$\dot{a}_i$	3×1 vector of the transformer phase turns ratio.
bf	Relevant bifurcation nodes.
de	Describing nodes.
e	Edge nodes.
$f_h(P_h)$	Relationship between active and reactive powers for the h-th category.
in	Nodes other than the describing ones.
n_c	Number of categories of prosumers.
n_{eq}	Sum of the number of phases in all de busses.
n_f	Number of branches in the f-th feeder.
n_h	Number of prosumers in the h–th category.
n_{LA}	Sum of the number of phases in all Load Area busses.
$p^*_{h,k}$, $q^*_{h,k}$	Fixed share of the active and reactive power injection by the k-th prosumer in the h-th category.
$\bar{I}^s_i$, $\bar{I}^r_i$	3×1 vectors of the input (at the sending bus) and output (from the receiving bus) phase currents for the i-th branch.

The associate editor coordinating the review of this manuscript and approving it for publication was Lin Zhang.

$\bar{J}$	Injected currents.
$\bar{J}^{ext}$	Currents from the outside of the Load Area.
$\bar{J}^{p}$	Prosumers' injected currents.
$\bar{J}^{p}_{i\_\phi}$	Prosumers' injected current at the ϕ–th phase of the i–th bus.
P_h	Active power injection of the h-th category.
$P_{h,k}$, $Q_{h,k}$	Active and reactive power injection by the k-th prosumer in the h-th category.
$P^{inj}_{i\_\phi}$, $Q^{inj}_{i\_\phi}$	Active and reactive power injections in the ϕ-th phase of the i–th bus.
P_L	Active power consumption of the pure load prosumer's category.
$\dot{T}_i$	6×6 matrix for the i-th branch.
$\bar{U}$	Nodal voltages.
$\bar{U}_{i\_\phi}$	Voltage of the ϕ–th phase of the i–th bus.
$\bar{U}^{s}_{i}$, $\bar{U}^{r}_{i}$	3×1 vectors of the phase voltages at the sending and receiving busses for the i-th branch.
$\bar{Y}$	Admittance matrix.
$\dot{Y}^{s}_{i}$, $\dot{Y}^{r}_{i}$	3×3 matrices of shunt admittances, sending and receiving sides, for the i-th branch.
$\dot{Z}_i$	3×3 matrix of series impedance for the i-th branch.

I. INTRODUCTION

Distribution systems are profoundly involved in the change of the electricity industry towards higher flexibility, accessibility, reliability, affordability. Changes involve architecture, planning, monitoring and control, the role of users, connectivity among areas, and exploitation of renewables.

The planning of distribution systems in the changing scenario is based on new approaches requiring a huge amount of operations simulations [1]; the decision-making support system benefits from the reduced computational times deriving from a compact (yet accurate) grid modeling. The required new monitoring and control functionalities make available a very large amount of information [2], [3]; not all this information needs a detailed consideration, and a significant reduction in the related treatment burden can be achieved by considering only the strictly relevant one [4]. The need for a reduced representation of distribution grids is found also in real-time simulations useful to utilities to understand the operational behavior of physical devices without interfering with the actual grid [5].

To get a model of a distribution system that is accurate as needed without being unduly detailed, the concept of Load Area (LA) can be usefully adopted; a LA is a group of prosumers/nodes whose power injection has a similar impact on the operating conditions of the grid. Generally speaking, a LA is a subgrid; nevertheless, a LA can comprise a whole distribution grid [6]. With the adoption of the LA concept, only the relevant information can be selected; a compact yet accurate representation of the relationship between the relevant quantities can be derived as a reduced representation of the LA [7].

Network reduction is a classic topic in power systems [8], and is regularly revisited. Most methods have been developed for transmission systems; recently, many papers have been devoted to the simplification of the modeling of distribution networks. The present work is focused on distribution systems within the LA approach, which allows identifying the homogeneous parts of the grid whose representation can be simplified by a reduced equivalent model.

Compared to [1], in the current study lines are fully represented including line charging capacitances, and injections are modeled as powers and not currents. In [4], unbalanced laterals are reduced to the three-phase main feeders, while in this study the reduction is not focused on feeders, whose representation can be further compacted, and unbalanced busses can be retained as representative busses if needed. Reference [5] proposes a Montecarlo approach to reduce the grid, while our approach is non-iterative thanks to the eigenvalue sensitivities [9], [10] the LA approach is based upon. Reference [11] proposes a general network reduction method that groups nodes based on congestions only, while the current study also considers voltage issues and is specialized for unbalanced radial distribution systems. In [12], a network segment between two relevant busses is replaced by a two-port non-linear network; many busses have to be kept in the reduced model which is not the case in the current study. In [13], admittance matrix inversion is required for both the original and reduced network, and there is a choice to be made for the reduced impedance matrix as it is not unique; in the present study, there is no matrix inversion and no choice is required.

In this paper, a method to get the equivalent reduced modeling of an unbalanced radial distribution network is presented, starting from the identification process of LA subgrids proposed in [14]. The method is based on a specialized approach, which allows obtaining the reduced representation in a computationally efficient way for large grids. The method is made of a two-stage backward-forward (b&f) graph navigating technique and builds on a generalization of the description of one- and two-phase branches.

This work contributes to the existing literature on network reduction mainly with:

- uniform treatment of all busses, allowing to keep as representative busses also one- and two-phase ones;
- no requirement for admittance matrix inversion;
- exploitation of the radiality of the distribution grid to get a reduced representation;
- retention of the radiality in the reduced model.

The details of the method are presented, and the reduced relationships among relevant voltages/currents are obtained. The method is applied to five test cases of different sizes, highlighting the computational issues related to the reduced network representation and solution.

II. LOAD AREA - OVERVIEW

The LA concerns the management of DER flexibility, firstly proposed in the ADDRESS project [15] which was focused on the exploitation of the flexibility provided by small prosumers connected to low voltage distribution systems. A LA is a group of prosumers/nodes whose power injection has a similar impact on the distribution grid operating conditions; a whole distribution network can be seen as a composition of LAs.

The identification of a LA requires the consideration of the relevant operating limitations in the grid, the evaluation of the impact of the nodal injection on the relevant operating issues, the clustering of the nodes with close values of the impact factors. The above process is described in [7], [16] for balanced radial distribution systems, and in [14] for unbalanced radial systems.

Once identified, a LA can be represented with a reduced model, which accounts for the power injections by prosumer categories within the LA and describes the grid within the LA with a reduced model. The reduced models of the LAs are then composed to get the reduced model of the whole grid. For unbalanced systems, the representation of a LA is briefly recalled in the following; the reader is referred to [14] for more details.

A. PROSUMERS

In a given LA, similar prosumers (residential, commercial, etc.) are grouped in categories [7], [17]. The active power injection by the k-th prosumer in the h-th category can be assumed to be a fixed share of the active power injection of the whole category:

$$P_{h,k} = p^*_{h,k} P_h. \tag{1}$$

The reactive power injection by the same prosumer can be put as:

$$Q_{h,k} = q^*_{h,k} f_h(P_h) P_h; \tag{2}$$

for example, for a pure load category it would be:

$$q^*_{h,k} = \tan\varphi^*_{h,k} p^*_{h,k}, \quad f_h(P_h) = 1, \ h \equiv \text{ pure loads}. \tag{3}$$

The relationships between active and reactive powers for different prosumers' categories can be found in [14].

B. NODAL INJECTIONS

In the remaining of the paper, the terms proposed in [18] are used: a ''node'' is a single phase in a bus, and a ''bus'' is a group of nodes (one to three).

The prosumers' injected current in the ϕ–th phase of the i–th bus can be expressed as:

$$\begin{aligned} \bar{J}^p_{i\_\phi} &= \frac{P^{inj}_{i\_\phi} - j\, Q^{inj}_{i\_\phi}}{\widehat{U}_{i\_\phi}} \\ &= \frac{1}{\widehat{U}_{i\_\phi}} \sum_{h=1}^{n_c} \begin{bmatrix} \pi^*_{i\_\phi,h} & -j\rho^*_{i\_\phi,h} \end{bmatrix} \begin{bmatrix} 1 \\ f_h(P_h) \end{bmatrix} P_h, \end{aligned} \tag{4}$$

where symbol $\widehat{\ }$ represents the complex conjugate.

In (4), it is:

$$\begin{aligned} P^{inj}_{i\_\phi} &= \sum_{h=1}^{n_c} \sum_{k=1}^{n_h} \pi_{i\_\phi,h,k} P_{h,k} \\ &= \sum_{h=1}^{n_c} P_h \sum_{k=1}^{n_h} \pi_{i\_\phi,h,k}\, p^*_{h,k} \\ &= \sum_{h=1}^{n_c} \pi^*_{i\_\phi,h} P_h, \quad \phi = 1,2,3, \\ Q^{inj}_{i\_\phi} &= \sum_{h=1}^{n_c} \sum_{k=1}^{n_h} \pi_{i\_\phi,h,k} Q_{h,k} \\ &= \sum_{h=1}^{n_c} f_h(P_h) P_h \sum_{k=1}^{n_h} \pi_{i\_\phi,h,k}\, q^*_{h,k} \\ &= \sum_{h=1}^{n_c} \rho^*_{i\_\phi,h} f_h(P_h) P_h, \quad \phi = 1,2,3, \\ \pi^*_{i\_\phi,h} &= \sum_{k=1}^{n_h} \pi_{i\_\phi,h,k} p^*_{h,k}, \\ \rho^*_{i\_\phi,h} &= \sum_{k=1}^{n_h} \pi_{i\_\phi,h,k} q^*_{h,k}, \\ \pi_{i\_\phi,h,k} &= \begin{cases} 1/\nu_{h,k} & \text{if the } k\text{–th prosumer of the } h\text{–th} \\ & \text{category is connected in the} \\ & i\text{–th grid bus to the } \phi - \text{th} \\ & \text{phase;} \\ 0 & \text{otherwise.} \end{cases} \end{aligned} \tag{5}$$

By assuming that voltages do not change too much with respect to a reference case:

$$\bar{U}_{i\_\phi} \approx \bar{U}^*_{i\_\phi}, \tag{6}$$

eq. (4) becomes:

$$\begin{aligned} \bar{J}^p_{i\_\phi} &\approx \frac{1}{\widehat{U}^*_{i\_\phi}} \sum_{h=1}^{n_c} \left(\pi^*_{i\_\phi,h} - j\rho^*_{i\_\phi,h} f_h(P_h)\right) P_h \\ &= \sum_{h=1}^{n_c} \dot{\alpha}_{i\_\phi,h} \begin{bmatrix} 1 \\ f_h(P_h) \end{bmatrix} P_h, \end{aligned} \tag{7}$$

where

$$\dot{\alpha}_{i\_\phi,h} = \frac{1}{\widehat{U}^*_{i\_\phi}} \begin{bmatrix} \pi^*_{i\_\phi,h} & -j\rho^*_{i\_\phi,h} \end{bmatrix}. \tag{8}$$

C. LOAD AREA NETWORK REPRESENTATION

A reduced model of the LA can be envisaged, which retains only some nodes/busses of the original network. Based on the results of the LA identification, phase voltages of the edge busses and the currents injected in them from the outside are relevant describing quantities to represent the LA. Retaining other busses within the LA can be necessary to preserve the radiality of the compact model (namely the bifurcations in the subtree connecting edge or other relevant nodes/busses [7]),

or for monitoring and control purposes (such as the busses where OLTC or voltage-controlled DG are installed, possibly aggregated as in [19]).

For a LA, injected currents are the sum of the prosumers' currents given by (7), and the currents from the outside accounting for the connection of the LA to the remainder of the grid:

$$\bar{J} = \bar{J}^{ext} + \bar{J}^{p} = \left[\begin{bmatrix} \bar{J}_e \\ 0 \end{bmatrix}\right] + \bar{J}^{p} = \begin{bmatrix} \bar{J}_{de} \\ 0 \end{bmatrix} + \bar{J}^{p}, \quad (9)$$

where the meaning of the symbols is apparent.

The well-known relationship between injected currents and nodal voltages based on nodal admittance matrix can be written as [14]:

$$\begin{aligned} \bar{J} = \dot{Y}\bar{U} \Rightarrow \begin{bmatrix} \bar{J}_{de} \\ 0 \end{bmatrix} + \sum_{h=1}^{n_c} \begin{bmatrix} \dot{A}_{de} \\ \dot{A}_{in} \end{bmatrix}_h \begin{bmatrix} 1 \\ f_h(P_h) \end{bmatrix} P_h \\ \simeq \begin{bmatrix} \dot{Y}_{de,de} & \dot{Y}_{de,in} \\ \dot{Y}_{in,de} & \dot{Y}_{in,in} \end{bmatrix} \begin{bmatrix} \bar{U}_{de} \\ \bar{U}_{in} \end{bmatrix}, \end{aligned} \quad (10)$$

where the meaning of symbols is apparent; the approximation embedded in (10) is due to the assumption (6).

A Gaussian elimination allows to get a representation of the LA network based only on *de* nodes/busses:

$$\bar{J}_{de} = \begin{bmatrix} \bar{J}_e \\ 0 \end{bmatrix} = \dot{Y}_{eq}\bar{U}_{de} - \sum_{h=1}^{n_c} \dot{\Gamma}_{eq,h} \begin{bmatrix} 1 \\ f_h(P_h) \end{bmatrix} P_h, \quad (11)$$

where

$$\begin{aligned} \dot{Y}_{eq} &= \dot{Y}_{de,de} - \dot{Y}_{de,in}\dot{Y}_{in,in}^{-1}\dot{Y}_{in,de}, \\ \dot{\Gamma}_{eq,h} &= \dot{A}_{de,h} - \dot{Y}_{de,in}\dot{Y}_{in,in}^{-1}\dot{A}_{in,h}, \end{aligned} \quad (12)$$

with

$$\begin{aligned} dim\{\dot{Y}_{eq}\} &= n_{eq} \times n_{eq}, \\ dim\{\dot{\Gamma}_{eq,h}\} &= n_{eq} \times 2. \end{aligned} \quad (13)$$

It is noteworthy that this general formulation allows to retain as *de* busses also unbalanced busses, as phases are explicitly taken into account and represented.

The approximation coming from (6) can be reduced by taking into account the actual value of phase voltages of *de* busses:

$$\bar{J}_{de} = \dot{Y}_{eq}\bar{U}_{de} - diag\left\{\frac{\widehat{U}_{de}^{*}}{\widehat{U}_{de}}\right\} \sum_{h=1}^{n_c} \dot{\Gamma}_{eq,h} \begin{bmatrix} 1 \\ f_h(P_h) \end{bmatrix} P_h; \quad (14)$$

note that (14) is a load-flow equation (see [14] for more details). The approximation due to (6) for the eliminated *in* nodes still involves errors; but, they are very low and acceptable from a practical point of view (see [6], [7], [14]).

III. LOAD AREA REPRESENTATION FOR RADIAL NETWORKS - COMPONENTS

The general reduced model of a LA network expressed in (14) is not specialized to exploit specific aspects of the network, such as its topology.

In the paper, the approach proposed in [20] is adopted; it is conceived for radially operated distribution networks and avoids the calculation of the inverse in (12), fostering the computational efficiency in the case of large size grids. A two-stage graph navigation technique is adopted to get compact relationships among the quantities pertaining to the describing busses of the LA.

Any grid is obtained by assembling four basic elements: injections, branches, feeders, and forks; a brief description of the modeling of each one is recalled in the following. For one- and two-phase branches, a modeling is proposed to get the same formal representation as three-phase branches while not introducing any approximation.

A. INJECTIONS BY THE PROSUMERS

Injections by the prosumers are expressed by (7)-(8).

B. BRANCHES

Three-phase branches are described with a well-known π model. Virtual phases are added to one- and two-phase branches to get the same formal model as the three-phase ones; no approximation is introduced due to the addition. In this way, the notation is highly simplified, and information treatment as well. Indeed, the virtual connection is such that it simply mirrors the voltage(s) of the upstream phase(s) which is (are) missing downstream.

1) THREE-PHASE BRANCHES

A three-phase branch can be described by a three-phase π model connecting sending and receiving busses [21]; each phase is put in series with an ideal single-phase transformer that accounts for the possible regulation of voltage amplitude and/or phase shifting. The electrical circuit is depicted in Fig. 1. For the i-th branch, the following matrix relationship holds:

$$\begin{aligned} \begin{bmatrix} \bar{U}_i^s \\ \bar{I}_i^s \end{bmatrix} &= \dot{T}_i \begin{bmatrix} \bar{U}_i^r \\ \bar{I}_i^r - \bar{J}_i^p \end{bmatrix} \\ &= \dot{T}_i \begin{bmatrix} \bar{U}_i^r \\ \bar{I}_i^r \end{bmatrix} - \dot{T}_i \sum_{h=1}^{n_c} \begin{bmatrix} 0 \\ \dot{\alpha}_{i,h} \end{bmatrix} \begin{bmatrix} 1 \\ f_h(P_h) \end{bmatrix} P_h, \end{aligned} \quad (15)$$

where $\dot{T}_i$ is

$$\dot{T}_i = \begin{bmatrix} (I + \dot{Z}_i\dot{Y}_i^r)\, diag\{\dot{a}_i\} & \dot{Z}_i\, diag\{\dot{a}_i\} \\ (\dot{Y}_i^s + \dot{Y}_i^r + \dot{Y}_i^s\dot{Z}_i\dot{Y}_i^r)(diag\{\hat{a}_i\})^{-1} & (I + \dot{Y}_i^s\dot{Z}_i)(diag\{\hat{a}_i\})^{-1} \end{bmatrix}; \quad (16)$$

matrix $\dot{Y}_i^s$ contains half of the total line charging admittance, while matrix $\dot{Y}_i^r$ contains half of the total line charging admittance, possibly with the addition of the admittance of shunt elements located at the receiving node.

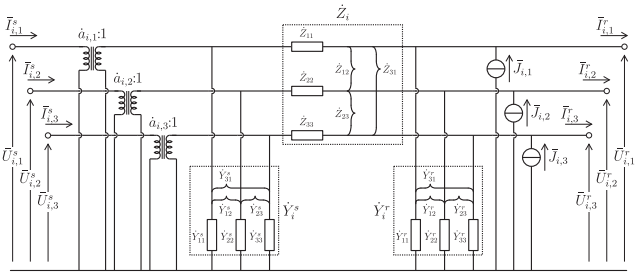

FIGURE 1. Generic *i*-th branch.

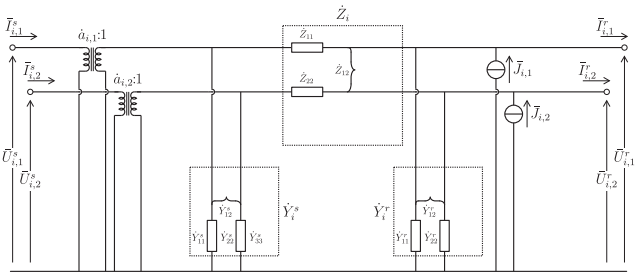

FIGURE 2. A two-phase branch.

2) ONE- AND TWO-PHASE BRANCHES

Let us consider a two-phase branch, and assume that phase 3 is the missing one; the circuit representation of such a line with a π model is depicted in Fig. 2. Let a virtual connection be added as phase 3 between the sending and the receiving busses, with the following characteristics:

$$\begin{aligned}
&\dot{Y}^s_{i,33} = 0, \quad \dot{Y}^r_{i,33} = 0,\\
&\dot{Y}^s_{i,13} = \dot{Y}^s_{i,31} = 0, \quad \dot{Y}^r_{i,13} = \dot{Y}^r_{i,31} = 0,\\
&\dot{Y}^s_{i,23} = \dot{Y}^s_{i,32} = 0, \quad \dot{Y}^r_{i,23} = \dot{Y}^r_{i,32} = 0,\\
&\dot{Z}_{i,31} = \dot{Z}_{i,32} = 0,\\
&\dot{Z}_{i,13} = \text{any value},\\
&\dot{Z}_{i,23} = \text{any value},\\
&\dot{Z}_{i,33} = \text{any value};
\end{aligned} \tag{17}$$

it is appropriate to put $\dot{Z}_{i,13} = \dot{Z}_{i,23} = 0$ in order to preserve the symmetry of matrix $\dot{Z}_i$. The virtual three-phase line has a π circuit representation reported in Fig. 3. With the values in (17), it follows that:

- for phase 3, with neither a load nor a downstream connection at the receiving bus, it is $\bar{I}^s_{i,3} = 0$ and $\bar{U}^s_{i,3} = \bar{U}^r_{i,3}$;
- there is no need for special values of $\dot{Z}_{3,3}$, such as 0 or very big.

The virtual three-phase branch has the same behavior as the actual two-phase one. Its representation differs from that of the actual branch due to the addition of a phase voltage, namely phase 3, at the receiving bus; this voltage simply mirrors that at the sending bus, with no modification of the voltages/currents of the actual phases of the actual branch. The model in Fig. 3 can be considered as the three-phase virtual equivalent of the actual two-phase branch.

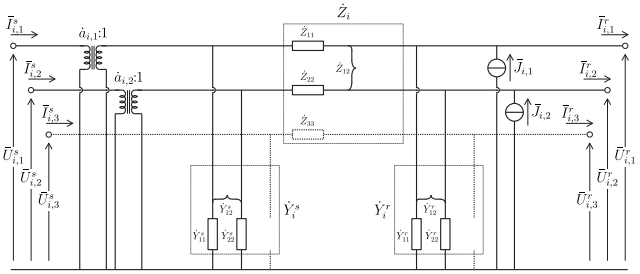

FIGURE 3. The virtual three-phase branch of a two-phase branch.

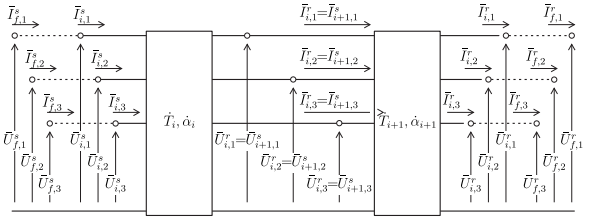

FIGURE 4. A feeder as a string of branches.

For a single-phase branch, a similar procedure can be adopted with the addition of two virtual connections between sending and receiving busses. Also, in this case, a three-phase virtual equivalent is obtained.

With the virtualization, all busses are treated in the same, uniform way in the specialized method; the feature of the general formulation in Sect. II-C of possibly retaining as *de* busses also one- and two-phase busses is maintained.

C. FEEDERS

A feeder is an ordered sequence of branches, such as the one in Fig. 4. For two subsequent branches of a feeder, it is:

$$\begin{aligned}
\bar{U}^r_i &= \bar{U}^s_{i+1},\\
\bar{I}^r_i &= \bar{I}^s_{i+1}.
\end{aligned} \tag{18}$$

For the entire f-th feeder, the recursive application of Eqs. (15) and (18) results in

$$\begin{bmatrix} \bar{U}^s_f \\ \bar{I}^s_f \end{bmatrix} = \dot{\Theta}_f \begin{bmatrix} \bar{U}^r_f \\ \bar{I}^r_f \end{bmatrix} - \sum_{h=1}^{n_c} \dot{\Gamma}_{f,h} \begin{bmatrix} 1 \\ f_h(P_h) \end{bmatrix} P_h, \tag{19}$$

with

$$\begin{aligned}
\dot{\Theta}_f &= \prod_{i=1}^{n_f} \dot{T}_i,\\
\dot{\Gamma}_{f,h} &= \sum_{i=1}^{n_f} \prod_{j=1}^{i} \dot{T}_j \begin{bmatrix} 0 \\ \dot{\alpha}_{i,h} \end{bmatrix}.
\end{aligned} \tag{20}$$

D. FORKS

For a fork with m output feeders, it holds that

$$\begin{aligned}
\bar{U}^r_0 &= \bar{U}^s_j, \quad \forall j = 1, \ldots, m\\
\bar{I}^r_0 &= \sum_{j=1}^{m} \bar{I}^s_j,
\end{aligned} \tag{21}$$

where the subscript '0' denotes the incoming feeder.

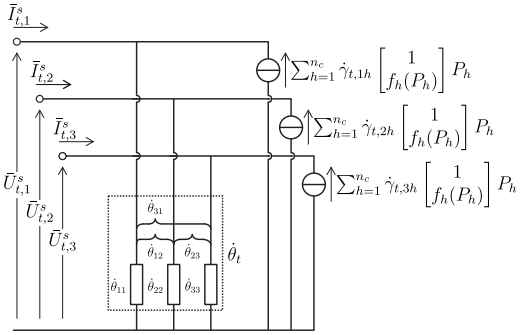

FIGURE 5. The reduced terminal branch.

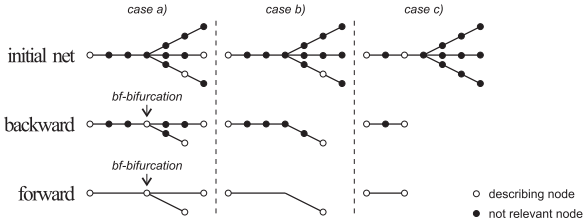

FIGURE 6. Reduction stages for the three relevant cases.

IV. LOAD AREA REPRESENTATION FOR RADIAL NETWORKS - MODEL REDUCTION

The models presented in Sect. III are adopted in combination with two-stage graph navigation to get the reduced modeling of the LA network.

The radiality of the network is exploited, and a radial reduced model is obtained for the LA. It is made of the describing nodes: edge nodes, other nodes to be explicitly considered for monitoring and control purposes, and relevant bifurcations [7], [20]. The radiality of the reduced LA model allows continuing using specialized algorithms and tools for radial distribution networks [22]–[26].

The two stages of the navigation technique are called backward and forward; they are described in the following.

A. BACKWARD STAGE

The backward stage starts from the terminal nodes and proceeds upstream through the graph towards the source bus. Voltage and current related to a terminal node are reported to the nearest upstream node.

For the t-th branch ending in a terminal node, it is $\bar{I}_t^r = 0$. From (15), (16), the following expression can be obtained:

$$\begin{aligned}\begin{bmatrix}\bar{U}_t^s\\ \bar{I}_t^s\end{bmatrix} &= \begin{bmatrix}\dot{T}_{t,11} & \dot{T}_{t,12}\\ \dot{T}_{t,21} & \dot{T}_{t,22}\end{bmatrix}\begin{bmatrix}\bar{U}_t^r\\ 0\end{bmatrix}\\ &\quad - \sum_{h=1}^{n_c}\begin{bmatrix}\dot{T}_{t,11} & \dot{T}_{t,12}\\ \dot{T}_{t,21} & \dot{T}_{t,22}\end{bmatrix}\begin{bmatrix}0\\ \dot{\alpha}_{t,h}\end{bmatrix}\begin{bmatrix}1\\ f_h(P_h)\end{bmatrix}P_h\\ &= \begin{bmatrix}\dot{T}_{t,11}\\ \dot{T}_{t,21}\end{bmatrix}\bar{U}_t^r - \sum_{h=1}^{n_c}\begin{bmatrix}\dot{T}_{t,12}\\ \dot{T}_{t,22}\end{bmatrix}\dot{\alpha}_{t,h}\begin{bmatrix}1\\ f_h(P_h)\end{bmatrix}P_h\\ &= \begin{bmatrix}\dot{T}_{t,11}\\ \dot{T}_{t,21}\end{bmatrix}\bar{U}_t^r - \sum_{h=1}^{n_c}\begin{bmatrix}\dot{\Gamma}_{t,h,1}\\ \dot{\Gamma}_{t,h,2}\end{bmatrix}\begin{bmatrix}1\\ f_h(P_h)\end{bmatrix}P_h, \quad (22)\end{aligned}$$

where

$$\begin{aligned}\dot{\Gamma}_{t,h,1} &= \dot{T}_{t,12}\,\dot{\alpha}_{t,h},\\ \dot{\Gamma}_{t,h,2} &= \dot{T}_{t,22}\,\dot{\alpha}_{t,h},\end{aligned} \quad (23)$$

and the meaning of $\dot{T}_{t,..}$ is apparent. By simple algebra, from (22), (23) it can be written:

$$\bar{U}_t^r = \dot{T}_{t,11}^{-1}\left(\bar{U}_t^s + \sum_{h=1}^{n_c}\dot{\Gamma}_{t,h,1}\begin{bmatrix}1\\ f_h(P_h)\end{bmatrix}P_h\right),$$

$$\begin{aligned}\bar{I}_t^s &= \dot{T}_{t,21}\dot{T}_{t,11}^{-1}\left(\bar{U}_t^s + \sum_{h=1}^{n_c}\dot{\Gamma}_{t,h,1}\begin{bmatrix}1\\ f_h(P_h)\end{bmatrix}P_h\right)\\ &\quad - \sum_{h=1}^{n_c}\dot{\Gamma}_{t,h,2}\begin{bmatrix}1\\ f_h(P_h)\end{bmatrix}P_h\\ &= \dot{\theta}_t\bar{U}_t^s - \sum_{h=1}^{n_c}\dot{\gamma}_{t,h}\begin{bmatrix}1\\ f_h(P_h)\end{bmatrix}P_h, \quad (24)\end{aligned}$$

with

$$\begin{aligned}\dot{\theta}_t &= \dot{T}_{t,21}\dot{T}_{t,11}^{-1},\\ \dot{\gamma}_{t,h} &= \dot{\Gamma}_{t,h,2} - \dot{T}_{t,21}\dot{T}_{t,11}^{-1}\dot{\Gamma}_{t,h,1}. \quad (25)\end{aligned}$$

Equation (24) indicates that the sending bus of a terminal branch sees an equivalent circuit made of an admittance in parallel with an injection, as in Fig. 5. These elements can be included in the description of the upstream branch as follows.

Let u denote the upstream branch; from (15) and (24), it is easy to show that

$$\begin{aligned}\begin{bmatrix}\bar{U}_u^s\\ \bar{I}_u^s\end{bmatrix} &= \begin{bmatrix}\dot{T}_{u,11} & \dot{T}_{u,12}\\ \dot{T}_{u,21} & \dot{T}_{u,22}\end{bmatrix}\begin{bmatrix}1 & 0\\ \dot{\theta}_t & 1\end{bmatrix}\begin{bmatrix}\bar{U}_u^r\\ 0\end{bmatrix}\\ &\quad - \sum_{h=1}^{n_c}\begin{bmatrix}\dot{\Gamma}^*_{u,h,1}\\ \dot{\Gamma}^*_{u,h,2}\end{bmatrix}\begin{bmatrix}1\\ f_h(P_h)\end{bmatrix}P_h, \quad (26)\end{aligned}$$

where

$$\begin{aligned}\dot{\Gamma}^*_{u,h,1} &= \dot{T}_{u,12}(\dot{\alpha}_{u,h} + \dot{\gamma}_{t,h}),\\ \dot{\Gamma}^*_{u,h,2} &= \dot{T}_{u,22}(\dot{\alpha}_{u,h} + \dot{\gamma}_{t,h}). \quad (27)\end{aligned}$$

Equation (26) is formally similar to (22), meaning that the reduction process can continue. The reduction starts from terminals and ends when the receiving node of the upstream branch is a describing node (which has to remain explicitly represented). The entire backward stage ends when all terminals have been processed.

Figure 6 shows the three relevant cases of the location of the describing nodes and the results of the reduction at the end of the backward stage; note the presence of a *bf*-bifurcation in case *a*).

B. FORWARD STAGE

The forward stage continues the reduction process of the backward stage. Starting from the source bus and proceeding towards the terminals, the reduction operates on the feeders, eliminating all non-describing nodes between the describing ones (see Fig. 6).

TABLE 1. Mean times to get the compact representation and to solve the power-flow problem (max error = 10^{-6}).

			small	medium	large ×3	large ×5	large ×10
full	size	busses	15	124	371	617	1232
		nodes	38	256	765	1271	2536
	time to solve [s]	b&f	0.006	0.025	0.074	0.145	0.443
		classical N-R	0.012	0.226	3.220	12.226	109.895
reduced	size	busses	3	7	7	11	21
		nodes	9	21	21	33	63
	time to get [s]	by [14]	0.123	0.144	0.334	0.721	2.743
		new	0.650	0.651	0.653	0.734	1.127
	time to solve [s]	b&f	0.004	0.004	0.004	0.005	0.007

For a feeder between two describing nodes, Eqs. (19)–(20) hold and become

$$\begin{bmatrix} \bar{U}_f^s \\ \bar{I}_f^s \end{bmatrix} = \dot{\Theta}_f^\beta \begin{bmatrix} \bar{U}_f^r \\ \bar{I}_f^r \end{bmatrix} - \sum_{h=1}^{n_c} \dot{\Gamma}_{f,h}^\beta \begin{bmatrix} 1 \\ f_h(P_h) \end{bmatrix} P_h, \tag{28}$$

with

$$\begin{aligned} \dot{\Theta}_f^\beta &= \prod_{i=1}^{n_f} \dot{T}_i^\beta, \\ \dot{\Gamma}_{f,h}^\beta &= \sum_{i=1}^{n_f} \prod_{j=1}^{i} \dot{T}_j^\beta \begin{bmatrix} 0 \\ \dot{\alpha}_{i,h}^\beta \end{bmatrix}, \end{aligned} \tag{29}$$

where β is meant to refer to the reduced network obtained at the end of the backward stage. The results of the forward stage, which are those of the complete reduction process, are depicted in Fig. 6 for the three relevant cases.

Eventually, to reduce the approximation introduced by (6), the expression of the equivalent injected currents in (28) can be modified as follows (see (14)):

$$\begin{bmatrix} \bar{U}_f^s \\ \bar{I}_f^s \end{bmatrix} = \dot{\Theta}_f^\beta \begin{bmatrix} \bar{U}_f^r \\ \bar{I}_f^r \end{bmatrix} - \begin{bmatrix} diag\left\{\widehat{U}_f^{*r}/\widehat{U}_f^r\right\} & 0 \\ 0 & diag\left\{\widehat{U}_f^{*r}/\widehat{U}_f^r\right\} \end{bmatrix} \times \sum_{h=1}^{n_c} \dot{\Gamma}_{f,h}^\beta \begin{bmatrix} 1 \\ f_h(P_h) \end{bmatrix} P_h. \tag{30}$$

V. NUMERICAL RESULTS

The case studies illustrate the methods discussed in Sect. III-IV for grids of various sizes, which include pure loads and distributed generation (DG). Network data are derived from the IEEE Test feeder [27] and the OpenDSS Simulation Tool [18], and refer to unbalanced three-phase systems; balanced systems are treated in [20].

After the identification of the LAs (upon the procedure presented in [14]), the method of Sect. IV applies to obtain the radial reduced representation of the networks. The results illustrate the networks at the end of the backward stage and the end of the entire b&f reduction process, highlighting the successive reductions of the grid.

The errors in nodal voltages between the reduced model (with either (28) or (30)) and the complete one, for different values of the load both with and without DG, provide an estimate of the approximation introduced by the reduced model versus the loading conditions. When DG is considered, its total amount equals 20% of the total reference load; the number of DG generators is about 20% of network load busses and they are located in the 20% most loaded three-phases busses. Numerical tests with different sizes and locations of DG show voltage errors of the same magnitude as the ones presented in the following.

According to [4], the modeling error is judged admissible if it is less than the one due to the smallest tap changer step of OLTCs in the grid; for a 32-step voltage regulator with a range of a ±10% a one-step tap-change equals 0.006250 p.u.

A. SMALL-SIZE GRID

The small test grid is a realization of the IEEE 13-bus test feeder; Figure 7-a illustrates the network scheme, where the bus 670 is the equivalent load of the distributed load on line 632–671 and the bus rg60 includes the voltage regulators on the three phases [18]. It is assumed that the switch along the path 671-675 is closed and that the three-phase transformers are all wye-wye, with neutrals grounded. Assuming the relevance of voltage concerns only, the LA identification process results in the presence of three LAs (see also [14]), with only three describing busses *de*, the edges of the three LAs; they are the source, rg60, and 671 busses, highlighted in Fig. 7-b as empty blue circles.

The two-stage graph navigation technique of Sect. IV applies to find the describing relationships among the *de* busses. Figure 7-c illustrates the network resulting at the end of the backward stage; the absence of *bf*-bifurcations, in this case, is apparent. Finally, Figure 7-d shows the network resulting at the end of the entire process, with all *in* busses eliminated in the reduced representation.

Figure 8 reports in log scale the maximum errors in the nodal voltage (modulus) introduced by the models (28) or (30), for different values of the load with and without DG; the acceptability limit is indicated by a red dash-dot line. For each node, the voltage error is computed against the voltage

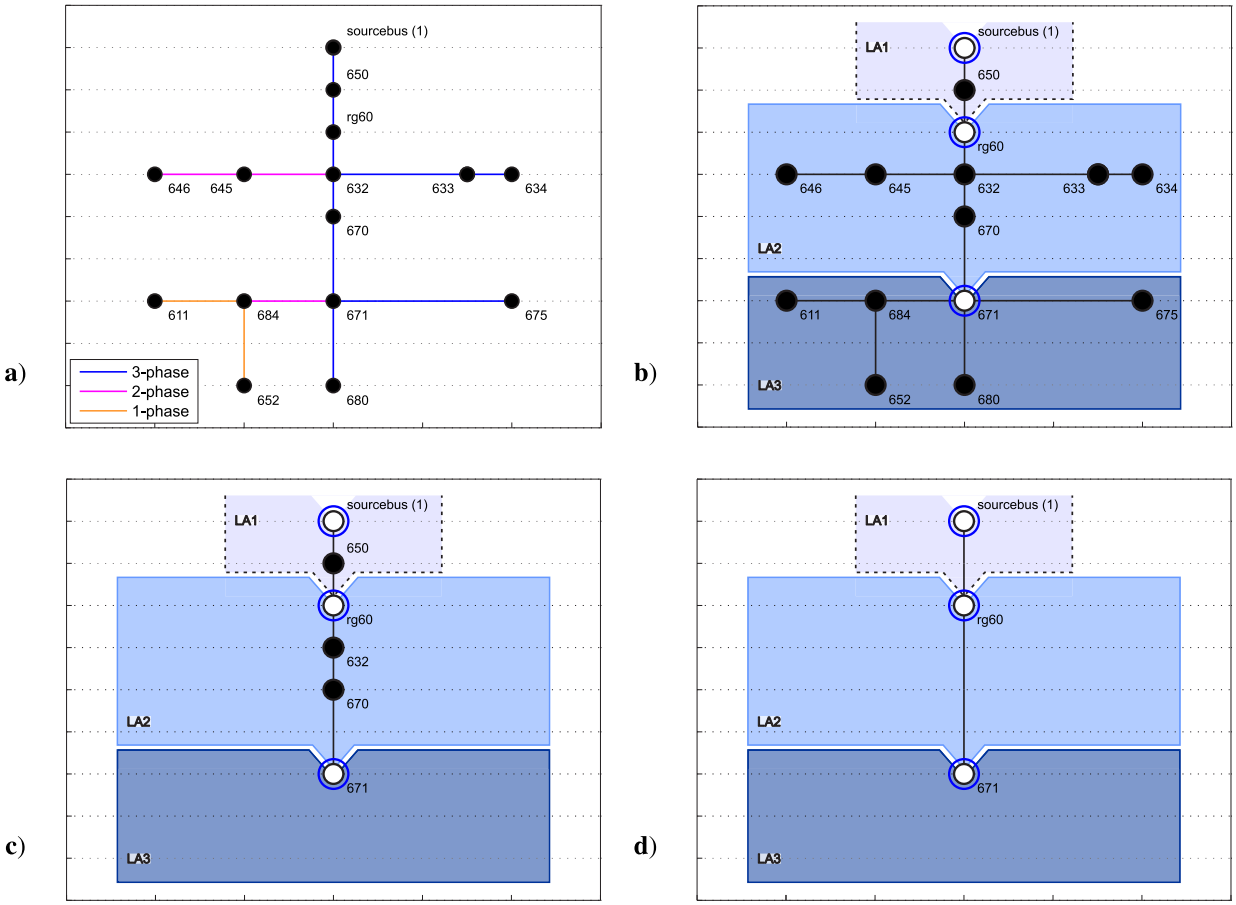

FIGURE 7. Small-size grid – (a) topology; (b) busses on the LA borders (empty circles); (c) grid after backward reduction; (d) grid after entire backward-forward reduction.

computed on the unreduced grid. Figure 8 shows that the maximum voltage error with (30) always assumes acceptable values, while with (28) it assumes much higher values and also non-admissible ones.

Table 1 shows some mean computational times, obtained with repeated runs on a desktop computer equipped with an Intel© Core™ i7 CPU 4780 with 32 GB of RAM run under Windows 10 64-bit operating system and Matlab R2016b. The time to get the reduced representation is evaluated for both the methods of [14] and the present one; the time to solve the load-flow is evaluated for the reduced model solved with a b&f method, and for the full model solved with a b&f method and a classical Newton-Raphson algorithm.

Results show that to get the reduced model for this small scale network the method [14] is preferable to the presented one; this is due to the time required to account for the network topology, which is relevant compared to the one of [14] in which only a small matrix needs to be inverted in (12).

The grid model obtained with the new method can be solved with the efficient b&f technique, which makes the new method preferred as concerns the time to solve the network.

B. MEDIUM-SIZE GRID

The second test network is obtained from the 123-bus IEEE test grid.

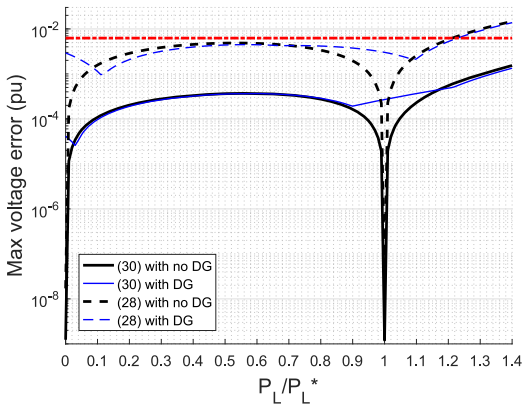

FIGURE 8. Max error in voltages for the small grid.

The representation of the network is depicted in Fig. 9-a, where the busses 9r, 25r, and 160r are added to represent the presence of the voltage regulators [18]. Also, for this grid, it is assumed that the three-phase transformers are all wye-wye, with neutrals grounded.

Assuming the presence of two overloaded lines, 23–25 and 97–101, and that the voltage is of concern, the LA identification process ends with five LAs (see [14]), with the five edge busses 149, 25, 101, 80 and the source bus, highlighted in

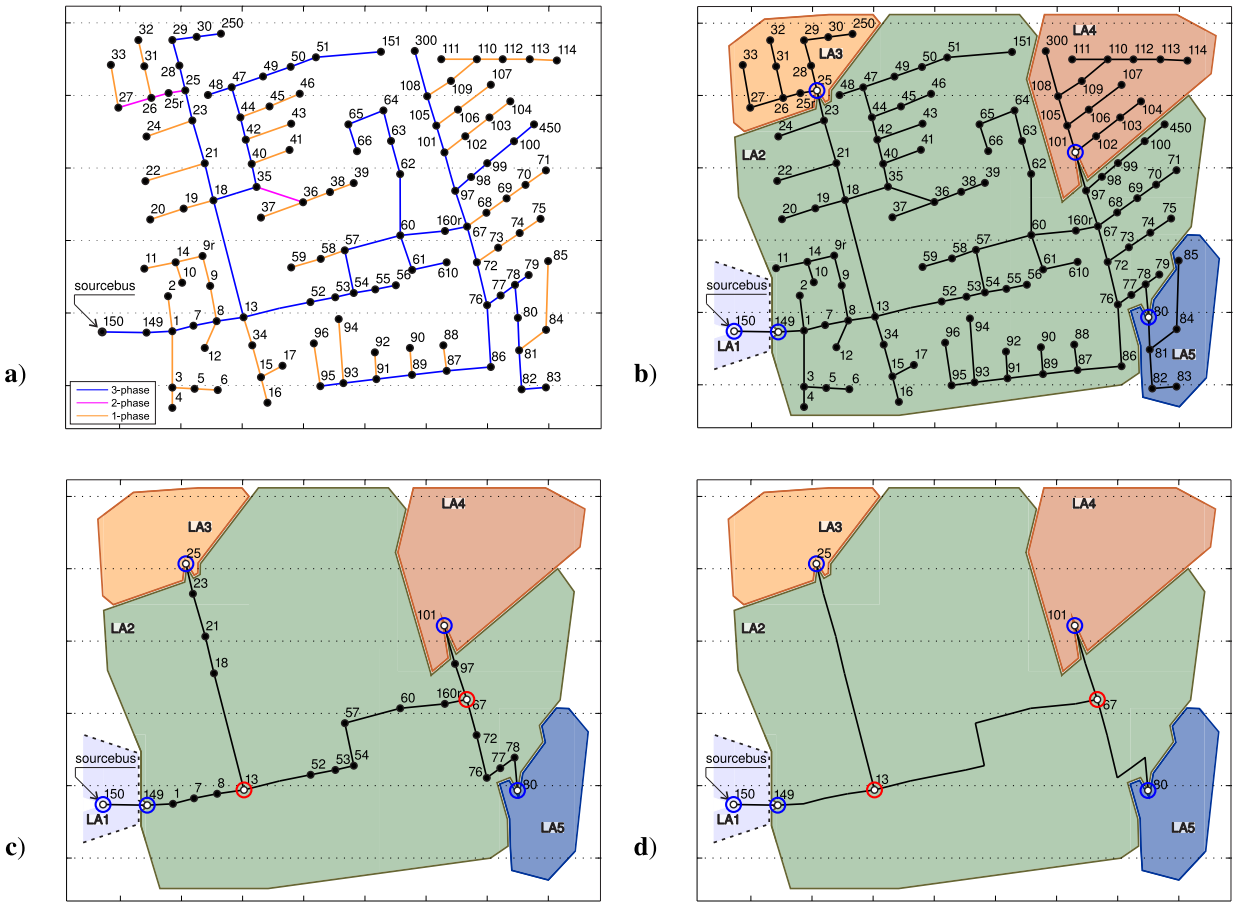

FIGURE 9. Medium-size grid – (a) topology; (b) busses on the LA borders (empty circles); (c) grid after backward reduction; (d) grid after entire backward-forward reduction.

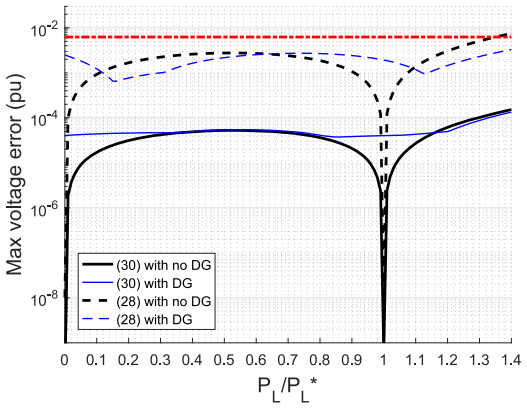

FIGURE 10. Max error in voltages for the medium-size grid.

Fig. 9-b as blue empty circles. Also, in this case, the methods of Sect. 3-IV are applied to get the describing relationships among the describing busses. The network resulting after the backward stage is depicted in Fig. 9-c; the presence of two *bf*-bifurcations (busses 13 and 67) is apparent (empty circles highlighted in red). The result of the forward stage is illustrated in Fig. 9-d; it shows seven describing nodes (5 edges + 2 *bf*-bifurcations).

Figure 10 reports in log scale the maximum errors in the nodal voltage (modulus) of the reduced models versus the total load, with and without DG. Also, in this case, it can be noticed that the maximum voltage errors with (30) are much lower than the errors with (28). Despite the size of the grid, the errors are smaller than the ones of the small-size grid; it is likely due to the lesser unbalance of the medium-size grid with respect to the small-size one, as confirmed by numerous numerical experiments.

Also, in this case, the computational time required to get the LA representation is in favor of the method [14] (see Tab. 1); indeed, also for this case, the size of the matrix to be inverted in (12) is too small to appreciate significant differences, while the time to describe the network structure is substantially the same as for the small grid. In contrast, the time to solve the power flow with the b&f technique applied to the grid obtained with the new method is consistently lower than the one for the original network (and similar to the one for the small grid).

C. LARGE-SIZE NETWORKS

The case study on larger networks is built by repeatedly replicating the IEEE 123 bus test grid (from the same origin),

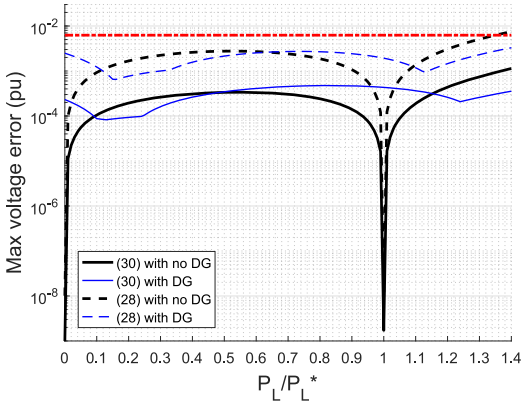

FIGURE 11. Max error in voltages for the large-size grid (×3, ×5, ×10).

to increase the overall number of busses while maintaining the structure of the original network. Specifically, the tests have been carried out by replicating the original network 3, 5, and 10 times. For simplicity, the identification of LAs is conducted assuming the relevance of voltage issues alone; this leads to the identification of only three busses for each network replica (150, 149, 80). No significant difference in the voltage errors emerged between the medium-size and large-size grids (see Fig. 10 and Fig. 11); in contrast, the time needed to solve the network appears deeply influenced by the grid size, in particular for the original model (see Tab. 1). The time required to obtain the reduced representation is still in favor of [14] for the cases ×3 and ×5 size networks, while the new method performs better for the biggest grid; this is because the time needed to invert the matrix in (12) becomes increasingly relevant. The computational time with the b&f technique is definitely in favor of the grid obtained with the new method.

D. A COMPARISON

As regards the time to get the reduced representation alone, it can be seen that the method [14] should be the preferred choice for small to moderate-size grids, while for big grids the new method would be preferred. On the other hand, the choice of the method to adopt could be driven not only by the time to get the reduced representation, but also by the time needed to solve the resulting network.

By looking at both the two aspects, the new method allows solving the reduced grid with the efficient b&f technique; then, the new method is by large the preferable one, as, for example, in planning studies where a large number of network solutions are required.

VI. CONCLUSION

In this paper, within the LA approach, a specialized method for obtaining a reduced representation of radial unbalanced distribution systems is proposed. The method is made of a two-stage graph navigation technique and is based on a generalization of the modeling of unbalanced one- and two-phase branches, which allows treating all busses in the same, uniform way. The method is applied to five unbalanced test cases of different sizes. The results confirm the viability of the proposed method, which is always the preferred choice for large grids; it has to be preferred also for small-to-medium grids if both the time to get the representation and the one to solve the grid are accounted for.

Future work will deal with the requirement of retaining additional nodes within the LA whose injection depends on/controls the voltage such as switching capacitors, OLTCs, DG inverters, and their possible aggregation.

REFERENCES

[1] Z. K. Pecenak, V. R. Disfani, M. J. Reno, and J. Kleissl, "Multiphase distribution feeder reduction," *IEEE Trans. Power Syst.*, vol. 33, no. 2, pp. 1320–1328, Mar. 2018.
[2] X. Lu, W. Wang, and J. Ma, "An empirical study of communication infrastructures towards the smart grid: Design, implementation, and evaluation," *IEEE Trans. Smart Grid*, vol. 4, no. 1, pp. 170–183, Mar. 2013.
[3] Y. Yan, Y. Qian, H. Sharif, and D. Tipper, "A survey on smart grid communication infrastructures: Motivations, requirements and challenges," *IEEE Commun. Surveys Tuts.*, vol. 15, no. 1, pp. 5–20, 1st Quart., 2013.
[4] A. B. Eltantawy and M. M. A. Salama, "A novel zooming algorithm for distribution load flow analysis for smart grid," *IEEE Trans. Smart Grid*, vol. 5, no. 4, pp. 1704–1711, Jul. 2014.
[5] A. Nagarajan, A. Nelson, K. Prabakar, A. Hoke, M. Asano, R. Ueda, and S. Nepal, "Network reduction algorithm for developing distribution feeders for real-time simulators," in *Proc. IEEE Power Energy Soc. Gen. Meeting*, Jul. 2017, pp. 1–5.
[6] G. M. Casolino and A. Losi, "Load area model accuracy in distribution systems," *Electric Power Syst. Res.*, vol. 143, pp. 321–328, Feb. 2017.
[7] G. M. Casolino and A. Losi, "Load areas in distribution systems," in *Proc. IEEE 15th Int. Conf. Environ. Electr. Eng. (EEEIC)*, Jun. 2015, pp. 1637–1642.
[8] J. B. Ward, "Equivalent circuits for power-flow studies," *Trans. Amer. Inst. Electr. Eng.*, vol. 68, no. 1, pp. 373–382, Jul. 1949.
[9] M. A. Laughton and M. A. El-Iskandarani, "On the inherent network structure," in *Proc. 6th PSCC*, Aug. 1978, pp. 188–196.
[10] A. Z. Gamm, I. I. Golub, A. Bachry, and Z. A. Styczynski, "Solving several problems of power systems using spectral and singular analyses," *IEEE Trans. Power Syst.*, vol. 20, no. 1, pp. 138–148, Feb. 2005.
[11] H. Oh, "A new network reduction methodology for power system planning studies," *IEEE Trans. Power Syst.*, vol. 25, no. 2, pp. 677–684, May 2010.
[12] A. P. Reiman, T. E. McDermott, M. Akcakaya, and G. F. Reed, "Electric power distribution system model simplification using segment substitution," *IEEE Trans. Power Syst.*, vol. 33, no. 3, pp. 2874–2881, May 2018.
[13] Z. K. Pecenak, V. R. Disfani, M. J. Reno, and J. Kleissl, "Inversion reduction method for real and complex distribution feeder models," *IEEE Trans. Power Syst.*, vol. 34, no. 2, pp. 1161–1170, Mar. 2019.
[14] G. M. Casolino and A. Losi, "Load areas in radial unbalanced distribution systems," *Energies*, vol. 12, no. 15, p. 3030, Aug. 2019. Accessed: Sep. 16, 2020. [Online]. Available: https://www.mdpi.com/1996-1073/12/15/3030
[15] R. Belhomme, R. Cerero Real De Asua, G. Valtorta, A. Paice, F. Bouffard, R. Rooth, and A. Losi, "ADDRESS—Active demand for the smart grids of the future," in *Proc. CIRED Seminar, SmartGrids Distrib.* Frankfurt, Germany: IET, Jun. 2008, pp. 1–4.
[16] G. M. Casolino and A. Losi, "Load area application to radial distribution systems," in *Proc. IEEE 1st Int. Forum Res. Technol. Soc. Ind. Leveraging Better Tomorrow (RTSI)*, Sep. 2015, pp. 269–273.
[17] P. Koponen, J. Ikaheimo, A. Vicino, A. Agnetis, G. De Pascale, N. R. Carames, J. Jimeno, E. F. Sanchez-Ubeda, P. Garcia-Gonzalez, and R. Cossent, "Toolbox for aggregator of flexible demand," in *Proc. IEEE Int. Energy Conf. Exhib. (ENERGYCON)*, Sep. 2012, pp. 623–628.

[18] *EPRI, OpenDSS Simulation Tool*. Accessed: Sep. 16, 2020. [Online]. Available: http://smartgrid.epri.com/SimulationTool.aspx
[19] Z. K. Pecenak, H. V. Haghi, C. Li, M. J. Reno, V. R. Disfani, and J. Kleissl, "Aggregation of voltage-controlled devices during distribution network reduction," *IEEE Trans. Smart Grid*, early access, Jul. 22, 2020, doi: 10.1109/TSG.2020.3011073.
[20] G. M. Casolino and A. Losi, "Specialized methods for the implementation of load areas in radial distribution networks," in *Proc. Power Syst. Comput. Conf. (PSCC)*, Jun. 2016, pp. 1–7.
[21] W. H. Kersting, *Distribution System Modeling and Analysis*. Boca Raton, FL, USA: CRC Press, 2012.
[22] S. Ghosh and D. Das, "Method for load-flow solution of radial distribution networks," *IEE Proc. Gener., Transmiss. Distrib.*, vol. 146, no. 6, pp. 641–648, Nov. 1999.
[23] A. Losi and M. Russo, "Object-oriented load flow for radial and weakly meshed distribution networks," *IEEE Trans. Power Syst.*, vol. 18, no. 4, pp. 1265–1274, Nov. 2003.
[24] G. M. Casolino, M. Landolfi, A. Losi, and M. Russo, "A software environment for developing object-oriented applications in distribution management systems," in *Proc. EUROCON Int. Conf. Comput. Tool*, Nov. 2005, pp. 1457–1460.
[25] G. W. Chang, S. Y. Chu, and H. L. Wang, "An improved backward/forward sweep load flow algorithm for radial distribution systems," *IEEE Trans. Power Syst.*, vol. 22, no. 2, pp. 882–884, May 2007.
[26] U. T. Ramirez and J. H. Tovar Hernandez, "Efficiency analysis of load flow methods for balanced radial distribution systems," in *Proc. IEEE Int. Autumn Meeting Power Electron. Comput. (ROPEC)*, Nov. 2013, pp. 1–6.
[27] *IEEE PES Test Feeders*. Accessed: Sep. 16, 2020. [Online]. Available: http://sites.ieee.org/pes-testfeeders/resources/

GIOVANNI MERCURIO CASOLINO (Member, IEEE) received the graduate degree (Hons.) in electrical engineering and the Ph.D. degree in electrical engineering and information technology from the University of Cassino and Southern Lazio, Cassino, Italy, in 1999 and 2004, respectively. He is currently an Assistant Professor with the University of Cassino and Southern Lazio, where he teaches courses in the power systems area. He is a coauthor of international scientific publications on the modeling of distribution systems by load areas, the optimal management of the deregulated electricity market, the object-oriented methods for state estimation in distribution networks, and the unit commitment and voltage regulation in presence of distributed generation.

ARTURO LOSI was born in Naples. He received the Laurea and Ph.D. degrees in electrical engineering from the University of Naples. Since 1988, he has been working with the Faculty of Engineering, University of Cassino and LM, where he has also a Full Professor, since 2000. He carried out research and seminar activities in the USA and Hong Kong. He teaches courses in the power systems area. He carries research on modeling of, and optimization in, power systems. He has served as Chair of Department, a member of governing bodies of an international Consortium of research, and the Chair of an Italian Interuniversity Consortium.